Journal of Advances in Medical and Pharmaceutical Sciences
5(3): 1-18, 2016, Article no.JAMPS.22095
ISSN: 2394-1111

SCIENCEDOMAIN *international*
www.sciencedomain.org

MicroRNA Memory II: A Novel Scoring Integration Model for Prediction of Human Disease by MicroRNA/MicroRNA Quantum Multi-Interaction

Tatsunori Osone[1*], Masaru Yoshikawa[1] and Yoichi R. Fujii[1,2]

[1]Pharmaco-MiRNA Genomics, Advanced Pharmaceutical Science Center, Graduate School of Pharmaceutical Sciences, Nagoya City University, Nagoya, 467-8603, Japan.
[2]Retroviral Genetics Group, Advanced Pharmaceutical Science Center, Graduate School of Pharmaceutical Sciences, Nagoya City University, Nagoya, 467-8603, Japan.

Authors' contributions

This work was carried out in collaboration among all authors. Author TO collected and calculated all data, performed the statistical analysis, did the literature search and wrote the first draft of the manuscript. Author MY developed score. Author YRF designed the study, also wrote the manuscript, and also did the literature search. All authors read and approved the final manuscript.

Article Information

DOI: 10.9734/JAMPS/2016/22095
Editor(s):
(1) Hamdy A. Sliem, Internal Medicine, Suez Canal University, Egypt and College of Dentistry, Qassim University and EL-Jouf University, Saudi Arabia.
Reviewers:
(1) Eman Ali Toraih, Suez Canal University, Egypt.
(2) Olga A. Berillo, Al-Farabi Kazakh National University, Kazakhstan.
(3) Zhiheng Zhou, Guangzhou University, China.
Complete Peer review History: http://sciencedomain.org/review-history/12275

Original Research Article

Received 17th September 2015
Accepted 28th October 2015
Published 12th November 2015

ABSTRACT

Aims: To further investigate quantum characters of the microRNA (miRNA) gene as the disease memory device, we calculated neo-score tool for miRNA/miRNA multi-interaction. Since the potential miRNA/target interaction is not one-to-one correspondence; therefore, the network of miRNA/mRNA is too busy to achieve the goal of prognosis and diagnose human disease.
Methodology: Neo-score tool based on quantum and electrodynamics for miRNA/miRNA multi-interaction, which are Dynamic Nexus Score (DNS) and Electric Field Tangent score (EFTS) is compare with Context+ Score Change (CSC) on PolymiRTS database, an integrated platform of the functional impact of genetic polymorphisms in miRNA seed regions and miRNA target sites within 149 human disease.

**Corresponding author: E-mail: c152707@ed.nagoya-cu.ac.jp, fatfuji@hotmail.co.jp;*

Results: The DNS was correlated with CSC. Since the EFTS was mathematically functioned into the DNS, the function of the DNS to the EFTS was integrated together disease prediction on CSC. Further, a possibility was suggested in this context that miRNA/miRNA multi-interaction on the algorithmic function could be applied for specific discernment of disease without miRNA/target interaction complex.
Conclusion: MiRNA/miRNA multi-interaction may have an important role for prognostic and diagnostic technologies for human health. This is the first report demonstrating that miRNA memory would manage the etiologies of human diseases.

Keywords: Human disease; miRNA; quantum; mRNA; polymiRTS.

1. INTRODUCTION

Recently, the function of non-coding RNAs (ncRNAs) has been investigated intensely, because ncRNAs have a key role in almost all cellular processes [1-3]. The ncRNAs are classified according to their length and function. The operation of long ncRNAs, whose length is more than 200 nucleotides, remains unclear. However, one type of small ncRNAs, the microRNAs (miRNAs), have an important direct or indirect role in the post-transcriptional and occasionally transcriptional regulation of gene expression and are highly conserved in various species. The miRNAs are approximately 22 nucleotides long, and their function of down-regulating messenger RNAs (mRNAs) expression is predicted on the basis of their seed region, which consists of nucleotides 2–8 at the 5' end [4-6]. Competitive binding of the seed, target and competing endogenous RNAs regulates the protein expression level [7-9].

Various databases and miRNA target prediction tools are currently available. For instance, Target Scan identifies candidate miRNAs based on the strength of interaction between the seed region and target site of miRNAs. TargetScan introduced the Context+ Score value, which enables the selection of the most favorable target sites for miRNAs. Context+ Score value evaluates miRNA binding in the context of the entire 3'untranslated region (3'UTR) of the mRNA by summing contributions made by individual sites that are perfectly complementary to the miRNA seed [10]. Context+ Score value consists of the following six contributions: Site-type, 3' pairing, local AU nucleotides, position, target site abundance (TA) and seed-pairing stability (SPS) [10]. This value is calculated for one miRNA and one target region. Another database, miRBase (http://mirbase.org/), can be used to obtain mature miRNA sequences [11], and dbSNP collects data about human single nucleotide polymorphisms (SNPs) [12]. Because Target Scan, miRBase and dbSNP are only available independently to investigate miRNA/mRNA interactions and SNPs, a combined prediction tool was lacking for more complex prediction tasks. In 2014, Bhattacharya et al. integrated these three databases creating the PolymiRTS combined prediction tool [13-15]. PolymiRTS database 3.0 (PolymiRTS: http://compbio.uthsc.edu/miRSNP/) collects SNPs located in miRNAs and miRNA target sites that are verified experimentally. In addition, PolymiRTS contains numerous miRNA targets, which are implicated in human disease, and data about the interaction between miRNA seed regions and 3'UTRs of mRNAs. Context+ Score change (CSC) value is the Context+ Score value corrected with the effect of polymorphisms in the miRNA target sites and miRNA seed regions. Compared with references, a more negative CSC value indicates an increase in the binding strength of miRNA and mRNA. A specific mRNA is often targeted by the same miRNA at multiple sites. CSC represents the change in binding strength between multiple miRNAs and SNPs within the mRNAs.

RNA Wave 2000 Model is the model interpreted RNA information genes (Rigs) [16]. The RNA Wave 2000 Model has four pillars; 1) the Rigs as a mobile genetic element induce transcriptional and post-transcriptional silencing via networking-architecture; 2) the Rigs expand into the environmental cycle of life; 3) the Rigs can self-proliferate; 4) the Rigs have two types of information as resident and genomic ones. The RNA Wave 2000 Model describes a novel mechanism of miRNA regulation, which can be affected by environmental factors [17]. The coherent on the quantum direction in the high dimensions has been shown in the matrix with the miRNA qubit code; however, the coherent was unavailable to apply for challenging against miRNA/miRNA multi-interaction.

Previously, we developed from single miRNA/miRNA interaction to two new scores of represented multiple miRNA/miRNA interactions based on the RNA Wave 2000 Model. One is based on quantum [16] and the other is based on electrodynamics [18]. Quantum based score, Dynamic Nexus Score (DNS), and the electrodynamics based score, Electric Field Tangent score (EFTS), were compared with CSC because miRNA/miRNA interactions were not calculated by CSC. CSC was linearly correlated with DNS. DNS and EFTS were non-linearly associated with human disease independent of CSC. After gaining an insight into miRNA/miRNA multiple interactions using network prediction tools, we might use this information for tailored medical care.

2. METHODOLOGY

2.1 MiRNA and mRNA Databases

All CSC data placed in Disease and Traits were prepared from PolymiRTS. In PolymiRTS, the cut off value of <50 of miRNA in one target mRNA was used. The mature.fa file in miRBase was downloaded in Release 21: June 2014, miRNA counts: 28,645 entries from a downloading page. All 2,588 of human miRNAs were extracted. CSCs related with 2,297 mRNA of 149 disease are used in this study (Table 1).

2.2 The New Score of DNS and DNSC

The miR-ket code and single miRNA/miRNA superposition in matrix were described previously [17]. The DNS is equal to the sum of each mathematical clause of the direct product when two miRNA sequences were diagnosed as a vector. Therefore, the miRNA group was defined as *A*, number of miRNA in *A* as N, each element of *A* as $A_i\{\mathrm{i} = 0,1,2,\dots,\mathrm{N}-1\}$, A_i's length as M_i and sequence of each element as $A_{ij}\{\mathrm{j} = 0,1,2,\dots,23\}$.

$$\mathrm{DNS} = \sum_{j=0}^{M_i} A_{0j} \times \sum_{j=0}^{M_i} A_{1j} \times \dots \times \sum_{j=0}^{M_i} A_{(N-1)j} \quad (1,0)$$

The DNS (1,0) is shown as synergy between among miRNAs in our previous report. Next, δ DNS were calculated as a change of the DNS. When miRNA group element shown as A_x and sequence of A_x as $A_{xj}\{\mathrm{j} = 0,1,2,\dots,23\}$, δ DNS was expressed as follows,

$$\delta DNS = DNS - \frac{DNS}{\sum_{j=0}^{M_i} A_{xj}} \quad (1,1)$$

This equation was rearranged as follows (1,1).

$$\delta DNS = \frac{DNS\left(\sum_{j=0}^{M_i} A_{xj} - 1\right)}{\sum_{j=0}^{M_i} A_{xj}} \quad (1,2)$$

Furthermore, to simplify this calculation (1, 2) was defined as DNSC.

$$\mathrm{DNSC} = \frac{\log_e(\delta DNS)}{N} = \frac{1}{N}\left(\sum_{i=0}^{N-1}\left(\log_e\left(\sum_{j=0}^{M_i} A_{ij}\right)\right) + \log_e\left(\sum_{j=0}^{M_i} A_{xj} - 1\right) - \log_e\left(\sum_{j=0}^{M_i} A_{xj}\right)\right) \quad (1,3)$$

Table 1. The number of miRNA's target in PolymiRTS used in this study

Phenotype	Number of diseases	Number of targets	Number of significant correlation[a]
Tumor	39	350	125
prostate cancer		64	20
breast cancer		39	13
others		247	92
Neurodegeneration	24	375	126
bipolar disorder		69	18
schizophrenia		60	22
others		246	86
Bone and Muscle	15	150	65
rheumatoid arthritis		42	18
amyotrophic lateral sclerosis		23	6
others		85	41
Cardiovascular disease	15	170	61

Phenotype	Number of diseases	Number of targets	Number of significant correlation[a]
coronary heart disease		57	24
hypertension		24	6
others		89	31
Gastrointestinal disturbance	12	367	147
crohn's disease		137	43
inflammatory bowel disease		133	55
others		97	49
Immune disease	8	164	69
systemic lupus erythematosus		45	16
celiac disease		41	20
others		78	33
Infection	6	37	13
leishmaniosis		14	6
AIDS progression		9	4
others		14	3
Skin	6	90	37
vitiligo		49	19
psoriasis		22	13
others		19	5
Renal failure	5	54	20
chronic kidney disease		36	13
nephropathy		11	3
others		7	4
Others	19	540	222
Total	149	2297	885

[a]*Significance of Dynamic Nexus Score Change and Context+ Score Change correlation. p<0.05*

2.3 The New Score of EFTS

Although the DNSC is the score that quantized the quantum energy in each base of miRNA, the new score based on electrodynamics was further developed. The electric field vector as *E*1 in any coordinate (x, y) to receive from electric charge Q in coordinate (X, Y) was expressed as follows.

$$\overrightarrow{E1} = \mathrm{k}\frac{\mathrm{Q(x-X)}}{\{(\mathrm{x-X})^2+(\mathrm{y-Y})^2\}^{\frac{3}{2}}}\vec{x} + \mathrm{k}\frac{\mathrm{Q(y-Y)}}{\{(\mathrm{x-X})^2+(\mathrm{y-Y})^2\}^{\frac{3}{2}}}\overrightarrow{y} \qquad (2,0)$$

When the number of electric charge increases, the electric field vector is demanded in the sum of the vector like the following expression as *E*2. The total number as N, each electric charge as $\mathrm{Q_i}$, each coordinate as $(\mathrm{X_i}, \mathrm{Y_i})\{\mathrm{i} = 0,1,2, \dots, \mathrm{N}-1\}$ was used as follows.

$$\overrightarrow{E2} = \mathrm{k}\sum_{i=0}^{N-1}\frac{\mathrm{Q_i(x-X_i)}}{\{(\mathrm{x-X_i})^2+(\mathrm{y-Y_i})^2\}^{\frac{3}{2}}}\vec{x} + \mathrm{k}\sum_{i=0}^{N-1}\frac{\mathrm{Q_i(y-Y_i)}}{\{(\mathrm{x-X_i})^2+(\mathrm{y-Y_i})^2\}^{\frac{3}{2}}}\vec{y} \quad (2,1)$$

With regard to a Watson-Crick and wobble base pair, the hydrogen atom (Fig. 1, H; red circle), the nitrogen atom non; blue circle) and the oxygen atom (Fig. 1, O; blue circle) were marked. And then, the ionic charges of H, N and O were defined as +1, -1 and -1, respectively. Adenine (Fig. 1A; 1, -1, 1), uracil (Fig. 1B; -1, 1, -1), guanine (Fig. 1C; -1, 1, 1) and cytosine (Fig. 1D; 1, -1, -1) were used in electric field vectors as the charges of nucleotides for computation of EFTS.

Further, (2,1) applied for miRNA. MiRNA sequence was defined as $A_i\{\mathrm{i} = 0,1,2, \dots, \mathrm{M}\}$ and charge of each A_i as $A_{ij}\{j = 0,1,2\}$. Coordinates of A_{ij} was shown as $(\mathrm{X_{ij}}, \mathrm{Y_{ij}})$, electric field vector E3 was expressed as follows.

$$\overrightarrow{E3} = \mathrm{k}\sum_{i=0}^{M}\sum_{j=0}^{2}\frac{A_{ij}\mathrm{(x-X_{ij})}}{\left\{\left(\mathrm{x-X_{ij}}\right)^2+\left(\mathrm{y-Y_{ij}}\right)^2\right\}^{\frac{3}{2}}}\vec{x} + \mathrm{k}\sum_{i=0}^{M}\sum_{j=0}^{2}\frac{A_{ij}\mathrm{(y-Y_{ij})}}{\left\{\left(\mathrm{x-X_{ij}}\right)^2+\left(\mathrm{y-Y_{ij}}\right)^2\right\}^{\frac{3}{2}}}\vec{y} \qquad (2,\ 2)$$

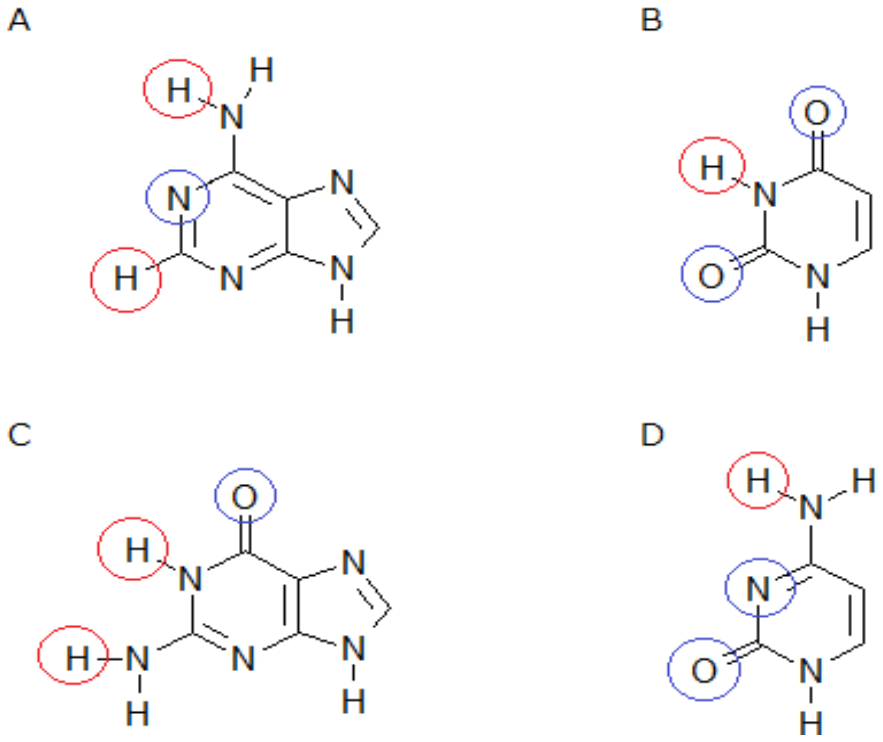

Fig. 1. EFTS related atoms in the nucleotide

In this formula, miRNA sequence was circularized in this model and (x, y) was any optional point.

The X ingredient (E_x) and the Y (E_y) ingredient of the electric field vector were separated as follows.

$$\overrightarrow{E_x} = \mathrm{k}\sum_{i=0}^{M}\sum_{j=0}^{2}\frac{A_{ij}(\mathrm{x}-\mathrm{X_{ij}})}{\left\{(\mathrm{x}-\mathrm{X_{ij}})^2+(\mathrm{y}-\mathrm{Y_{ij}})^2\right\}^{\frac{3}{2}}}\vec{x} \qquad (2,3)$$

$$\overrightarrow{E_y} = \mathrm{k}\sum_{i=0}^{M}\sum_{j=0}^{2}\frac{A_{ij}(\mathrm{y}-\mathrm{Y_{ij}})}{\left\{(\mathrm{x}-\mathrm{X_{ij}})^2+(\mathrm{y}-\mathrm{Y_{ij}})^2\right\}^{\frac{3}{2}}}\vec{y} \qquad (2,4)$$

The miRNA group as *A*, each element of $\overrightarrow{E_x}$ and $\overrightarrow{E_y}$ of A as $\overrightarrow{E_{\mathrm{i}x}}$ and $\overrightarrow{E_{\mathrm{i}y}}\{\mathrm{i}=0,1,2,\ldots,\mathrm{N}-1\}$, respectively. Total electric field vector E4 was expressed as follows.

$$\overrightarrow{E4} = \sum_{i=0}^{N-1}\overrightarrow{E_{\mathrm{i}x}} + \sum_{i=0}^{N-1}\overrightarrow{\mathrm{E_{iy}}} \qquad (2,5)$$

The radius of miRNA was defined as 50 units and one unit was corresponding to a lattice. The electric field was expressed at lattice points. The coordinate of lattice point was defined as $(\mathrm{x}_{kl}, y_{\mathrm{kl}})\{\mathrm{k}=-50,\ldots,0,\ldots,50;\ \mathrm{l}=-50,\ldots,0,\ldots,50\}$ and each ingredient of the electric field vector as $\overrightarrow{E_{klx}}$ and $\overrightarrow{E_{kly}}$. Tangential value when the electric field vector in each coordinates was defined as Electric Field Tangent score (EFTS). The formula is as follows.

$$\mathrm{EFTS_1} = \frac{\sum_{k=-50}^{50}\sum_{l=-50}^{50}\overrightarrow{\mathrm{E}_{kly}}}{\sum_{k=-50}^{50}\sum_{l=-50}^{50}\overrightarrow{\mathrm{E}_{klx}}} \qquad (2,6)$$

Further, $\mathrm{EFTS_1}$ (2, 6) in a miRNA were changed to $\mathrm{EFTS_2}$ in multiple miRNAs and the number of miRNA was shown as N.

$$\mathrm{EFTS_2} = \frac{\sum_{n=0}^{N-1}\sum_{k=-50}^{50}\sum_{l=-50}^{50}\overrightarrow{\mathrm{E}_{nkly}}}{\sum_{n=0}^{N-1}\sum_{k=-50}^{50}\sum_{l=-50}^{50}\overrightarrow{\mathrm{E}_{nklx}}} \qquad (2,7)$$

In (2,7), a component of electric field vector in each miRNA was shown as $\overrightarrow{E_{nklx}}, \overrightarrow{E_{nkly}}\{\mathrm{n}=0,1,\ldots,\mathrm{N}-1\}$, EFTSC was derived from $\mathrm{EFTS_2}$ (2, 7). Next, EFTSC were calculated as a change of the EFTS.

$$\mathrm{EFTSC} = \frac{\sum_{n=0}^{N-1}\sum_{k=-50}^{50}\sum_{l=-50}^{50}\overrightarrow{\mathrm{E}_{nkly}}}{\sum_{n=0}^{N-1}\sum_{k=-50}^{50}\sum_{l=-50}^{50}\overrightarrow{\mathrm{E}_{nklx}}} - \frac{\sum_{n=0}^{N-1}\sum_{k=-50}^{50}\sum_{l=-50}^{50}\overrightarrow{\mathrm{E}_{nkly}} - \sum_{k=-50}^{50}\sum_{l=-50}^{50}\overrightarrow{\mathrm{E}_{klY}}}{\sum_{n=0}^{N-1}\sum_{k=-50}^{50}\sum_{l=-50}^{50}\overrightarrow{\mathrm{E}_{nklx}} - \sum_{k=-50}^{50}\sum_{l=-50}^{50}\overrightarrow{\mathrm{E}_{klX}}} \qquad (2,8)$$

2.4 Mathematical Functioning EFTSC into DNSC

From (1,0), the scalar product is corresponding to number of G, therefore, DNSC can be replaced for number of G. EFTSC was calculated by Fourier transformation as analogy of quantum computation. Mean of EFTSC, y and number of G (DNSC), x were functioned as follows,

$$y = \sum_{i=0}^{N-1}\sum_{j=0}^{N-1}\left(\cos\left(\frac{2\pi ij}{N}\right)\cos(ix) - \frac{\sin\left(\frac{2\pi ij}{N}\right)}{N}\sin(ix)\right) \quad (3,0)$$

3. RESULTS

3.1 Molecular Modeling of miRNA/miRNA Multi-Interaction

DNS and CSC analysis were performed to evaluate miRNA/miRNA multi-interaction in Age-related disease, bone and muscle disease, cardiovascular disease, endocrine disease, eye disease, genital disease, gastrointestinal disturbance, immune disease, infection, lifestyle-related disease, neurodegeneration, renal failure, respiratory disease, skin disease, tooth disease and tumors (Table S1). The number of significant correlation between DNS and CSC was shown in Table 1. The relations between DNS from quantum scoring of miRNA/miRNA interaction and CSC from the context of miRNA/the target seed of mRNA were investigated (Fig. 2). DNSCs (x-axis) and CSCs (y-axis) were plotted in the case of a RFX7 target mRNA for chronic lymphocytic leukemia (Fig. 2A). The means of CSCs and the values of DNSC were represented in the same panel of A and the correlation efficiency was calculated (Fig, 2B). R^2 was contained as 0.8488, therefore the average of CSCs was highly correlated to DNSCs. For all target mRNAs in all disease of this study, all correlation efficiencies were calculated between DNSCs and CSCs, and then P-values in Pearson correlation efficiency were represented (Fig. 2C). Gaussian distribution was observed. Under less than 1% of p-value were 391 (17%) of target, under less than 5% of p-value were 885 (39%) of target and under less than 10% of p-value were 1190 (52%) of target (Fig. 2D). Top 5 of linear relation ($p<0.01$) between DNSC and CSC were shown in Table 2. In age-related macular degeneration, SNP allele alteration of 3'UTR target of GLI3, MBL2 and ARMS2 were strongly correlated with DNSC. Significant correlations against truncating variants in SNPs of TXNDC16 transcript variant notv) 2, GRM7 tv1 and GREM1 tv1 were also observed in orofacial cleft. About coronary heart disease, three SNPs in HLA-DPA1 tv3, SLC22A3 and LAMC2 had the high relationship to DNSC. Crohn's disease was clearly implicated with SNPs of EHB1 tv3 and DNSC or PDLIM4 tv2 and DNSC. In the case of type 2 diabetes mellitus, PAX4, PLS1 tv2, MAP3K1 and CDC123 showed profound nexuses of DNSC. Further, DNS was allele-specifically correlated with SNPs of ST8SIA2, CREB5 tv3 and SRP72 in airflow obstruction, and CHRNA4 and IREB2 in chronic obstructive pulmonary disease SNPs of PCLO tv1, ESRRG tv4, STMN2 tv1 and GRM7 tv1 were significantly related with DNSC in neurodegeneration of the major category of human disease. These results indicate that miRNA/miRNA interaction computed by DNSs provides different functions for browsing and searching data about SNPs and human disease and would be important candidates for disease phenotype prediction and complex trait studies.

3.2 Relations among EFTSs, DNSCs and CSCs

When the electric field vector in EFTS was applied for nucleotides of miRNA, E3 vectors of each nucleotide as torus showed specific characters among miRNAs as example, miR-10a-5p, miR-27a-5p, miR-191-5p, miR-200a-5p, miR-573 and miR-592 (Fig. S2A). Further, under mathematically simulated condition, coherence state of two miRNAs, such as miR-27a-5p (stayed) and miR-573 (moving) was made as two scalars and E4 was presented as a torus in Hilbert space (Fig. S2B). Superposing state of two miRNA/miRNA interaction was identical among every prohibiting set of miRNA/miRNA interaction, which also be corresponding to identical points of miRNAs between the CSC in the x-axis (red), DNSC in the y-axis (green) and the EFTSC in the z-axis (blue) on Fig. 3A. Therefore, these scalar values were transformed for multi miRNA/miRNA coherence as binary annotation in consideration of Watson-Crick and wobble base pairings, and then EFTSC score was computed. To further improve the accuracy of miRNA/miRNA multi-interaction EFTSC was integrated into the relation between CSC and DNSC in chronic lymphocytic leukemia, RFX7 target (Fig. 3A and Fig. S3A). These data showed that CSCs have linear relation with DNSCs (See Pearson correlation coefficient in Table S1) but all CSCs were not related with EFTSCs. Increasing of target further computation was performed. A figure of three-dimensional plot of mRNA related to chronic lymphocytic leukemia,

11 targets were visualized in web (Fig. S3B). Next, in bladder cancer, breast cancer, chronic lymphocytic leukemia and colorectal cancer, the DNSC plotting was performed and DNSCs in each disease were shown in Fig. 3B. In three-dimensional plot of mRNA related with Fig. 3B (Fig. S3C), CSCs, DNSCs and EFTSCs were visualized. In the case of another disease, atopic dermatitis, bladder cancer, biliary obstruction and chronic pulmonary disease, the DNSCs were processed at the same way (Fig. 3C and Fig. S3D). All CSCs, all DNSCs and all EFTSCs did not show significant relation among them under summing up of targets or disease. Since we did not obtain the possible formula to make impact of miRNA/miRNA multi-interaction, DNSC was compared to EFTSC in chronic lymphocytic leukemia, RFX7 target (Fig. 3D). The number of G-base was plotted to EFTSC, non-linear regression analysis was performed (blue line) and non-liner relation was observed. By definition of DNSC, DNSC is uniquely determined number of G in miRNA. Therefore, we confirmed relation between EFTSC and DNS (by number of G in miRNA).

3.3 Function of EFTSCs by DNSCs

As by non-linear regression analysis with Fourier transformation, number of G (x) and EFTSC (y) had some formula, a formula was prepared to be functioned by DNSCs. About top 5 of linear relation between DNSC and CSC (Table 2), 4, 5 and 6 of G (x) were substitute for the formula (Table 3). In each number of G in a phenotype, the maximum (red) and the minimum (blue) values of average of EFTSCs were represented. Although Pearson correlation efficient did not identify the value of average of EFTSCs, non-linear curve was computed on the targets, APOBEC3A tv1, TMEM129 tv2, PSCA tv1, CCNE1, FGFR3 tv3, SLC14A1 tv1, TP63 tv5 and TP63 tv3 in the bladder cancer (Fig. 4A). In Table 3, the maximum and the minimum values were tremendously different among x=4, 5 and 6. Therefore, each value was adjusted from -100 to 100 to make it easy to compare. Next, the average of each non-linear data was calculated on the same target as described above in the bladder cancer (Fig. 4B). Similar processes were performed in bladder cancer, breast cancer, chronic lymphocytic leukemia and colorectal cancer (Fig. 4C). Further, in atopic dermatitis, biliary obstruction, bladder cancer and chronic obstructive pulmonary disease, non-linear analysis was done (Fig. 4D). These results indicate that function of EFTSC by DNSC specifically showed disease phenotype modes.

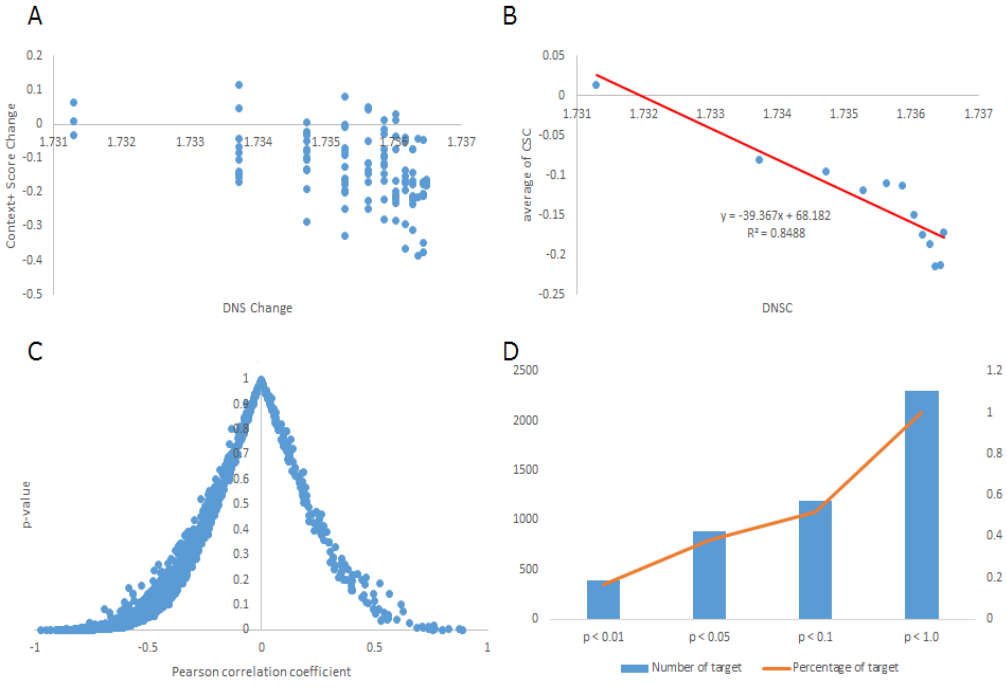

Fig. 2. Correlation between quantum score and the target seed

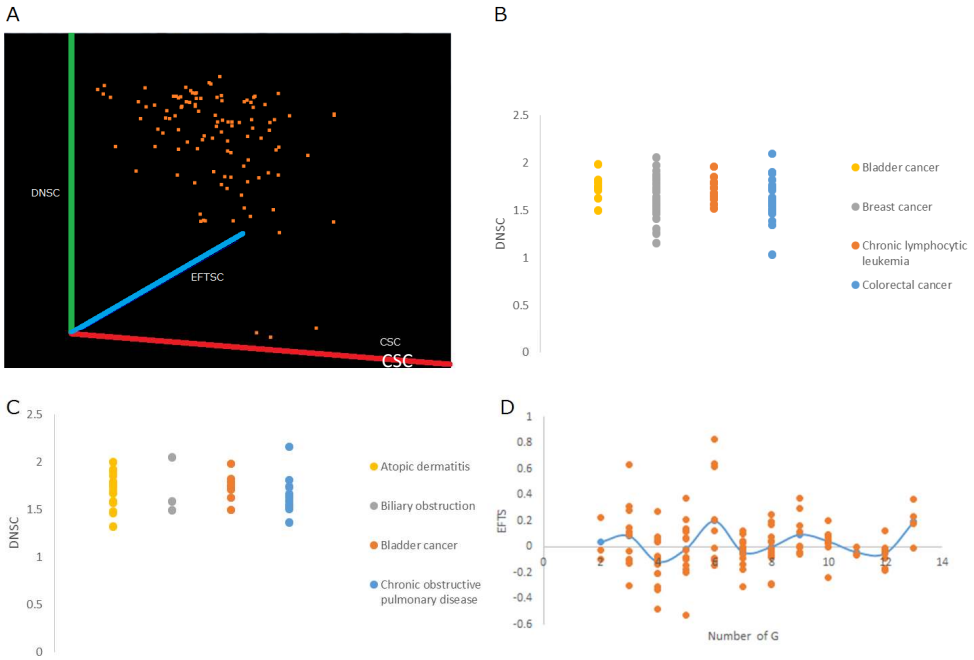

Fig. 3. Integration of EFTSC into relation between DNSC and CSC

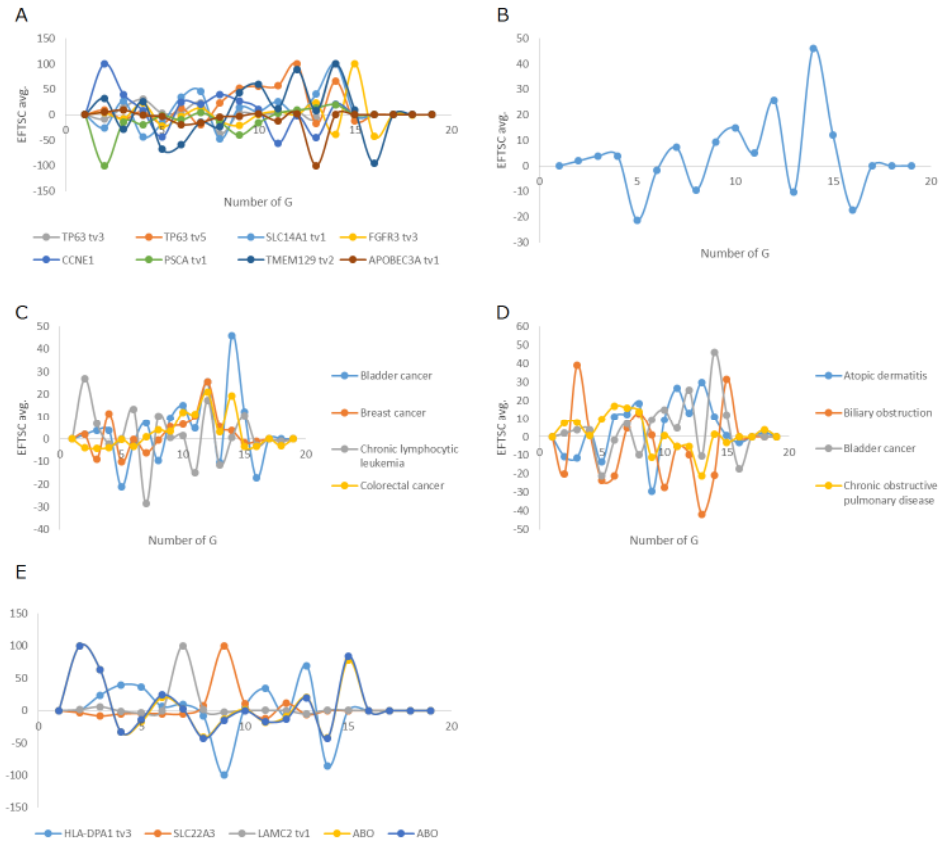

Fig. 4. Fourier transformation in EFTSC

Table 2. Top 5 of correlation between CSC and DNSC in each phenotype

Phenotype	Top 5 of linear-relation	p-value	Morphogenic target	Disease	RefSeqID
Age-related disease	-0.845	1.E-04	GLI3	age-related macular degeneration	NM_000168
	-0.835	4.E-04	MBL2	age-related macular degeneration	NM_000242
	-0.805	2.E-03	ARMS2	age-related macular degeneration	NM_001099667
	-0.792	4.E-04	ATCAY	aging	NM_033064
	-0.782	6.E-04	SH3BGRL2	aging	NM_174963
Bone and muscle	-0.898	1.E-05	TXNDC16 tv2	Orofacial clefts	NM_001160047
	0.890	2.E-05	POU3F1	Rheumatoid arthritis	NM_002699
	-0.860	3.E-04	IL23R	Ankylosing spondylitis	NM_144701
	-0.848	5.E-04	GRM7 tv1	Orofacial clefts	NM_000844
	-0.842	3.E-04	GREM1 tv1	Orofacial clefts	NM_013372
Cardiovascular disease	-0.825	5.E-04	HLA-DPA1 tv3	Coronary heart disease	NM_001242525
	-0.822	1.E-03	SLC22A3	Coronary heart disease	NM_021977
	-0.800	6.E-04	LAMC2 tv1	Coronary heart disease	NM_005562
	-0.794	7.E-04	ABO	Venous thromboembolism	NM_020469
	-0.794	7.E-04	ABO	Coronary heart disease	NM_020469
Gastrointestinal disturbance	-0.974	2.E-08	SPIB tv1	Primary biliary cirrhosis	NM_003121
	-0.901	3.E-05	EHBP1 tv3	Crohn's disease	NM_001142615
	-0.881	3.E-05	PDLIM4 tv2	Inflammatory bowel disease	NM_001131027
	-0.881	3.E-05	PDLIM4 tv2	Crohn's disease	NM_001131027
	-0.860	3.E-04	IL23R	Ulcerative colitis	NM_144701
Immune disease	-0.932	4.E-06	GHR tv12	Systemic lupus erythematosus	NM_001242462
	-0.879	8.E-05	TSHR tv1	Graves' disease	NM_000369
	-0.871	5.E-04	SLC15A4	Systemic lupus erythematosus	NM_145648
	-0.860	3.E-04	IL23R	Behcet's disease	NM_144701
	-0.845	1.E-04	GLI3	Allergic rhinitis	NM_000168
Infection	-0.881	7.E-05	RNF39 tv1	AIDS progression	NM_025236
	-0.860	3.E-04	IL23R	Leprosy	NM_144701
	-0.825	5.E-04	HLA-DPA1 tv3	Leishmaniasis	NM_001242525
	-0.794	7.E-04	ABO	Malaria	NM_020469
	-0.759	4.E-03	SCO1	Malaria	NM_004589

Lifestyle-related disease	-0.908	5.E-05	PAX4	Type 2 diabetes	NM_006193
	-0.891	2.E-04	PLS1 tv2	Type 2 diabetes	NM_002670
	-0.864	6.E-03	MAP3K1	Type 2 diabetes	NM_005921
	-0.854	2.E-04	DYRK1A tv5	Metabolic syndrome	NM_130438
	-0.848	2.E-04	CDC123	Type 2 diabetes	NM_006023
Neuro degeneration	-0.883	3.E-05	PCLO tv1	Major depressive disorder	NM_014510
	0.874	5.E-03	ARHGAP22	Conduct disorder	NM_001256026
	-0.855	2.E-04	ESRRG tv4	Major depressive disorder	NM_001134285
	-0.854	8.E-04	STMN2 tv1	Creutzfeldt-Jakob disease	NM_001199214
	-0.848	5.E-04	GRM7 tv1	Parkinson's disease	NM_000844
Renal failure	-0.928	2.E-06	CST3	Chronic kidney disease	NM_000099
	-0.889	1.E-04	CST9	Chronic kidney disease	NM_001008693
	-0.825	5.E-04	HLA-DPA1 tv3	Nephropathy	NM_001242525
	-0.804	5.E-04	AQP1 tv1	Nephrolithiasis	NM_198098
	-0.783	6.E-04	CYB561D1 tv5	Chronic kidney disease	NM_001134404
Respiratory	-0.828	1.E-04	CHRNA4	Chronic obstructive pulmonary disease	NM_000744
	-0.777	7.E-04	ST8SIA2	Airflow obstruction	NM_006011
	-0.773	7.E-04	CREB5 tv3	Airflow obstruction	NM_182899
	-0.715	1.E-02	IREB2	Chronic obstructive pulmonary disease	NM_004136
	-0.677	2.E-02	SRP72	Airflow obstruction	NM_006947
Skin	-0.860	3.E-04	IL23R	Psoriasis	NM_144701
	-0.825	5.E-04	HLA-DPA1 tv3	Vitiligo	NM_001242525
	-0.814	2.E-03	IL12B	Psoriasis	NM_002187
	-0.794	4.E-03	CDH23 tv2	Vitiligo	NM_052836
	-0.791	1.E-03	BNC2	Freckles	NM_017637
Tumor	-0.921	2.E-05	RFX7	Chronic lymphocytic leukemia	NM_022841
	-0.901	3.E-05	EHBP1 tv3	Prostate cancer	NM_001142615
	-0.896	8.E-05	CLDN11 tv1	Prostate cancer	NM_005602
	-0.865	1.E-04	TAP2 tv2	Lymphoma	NM_018833
	-0.864	6.E-03	MAP3K1	Breast cancer	NM_005921

Table 3. EFTSC of top 5 correlation between CSC and DNSC in each phenotype

Phenotype	Top 5 of linear-relation	x=4	x=5	x=6
Age-related disease	NM_000168	0.012	-0.016	0.007
	NM_000242	0.001	-0.022	-0.016
	NM_001099667	-0.099	0.021	-0.139
	NM_033064	-0.003	0.013	0.000
	NM_174963	-0.003	0.032	0.001
Bone and muscle	NM_001160047	-1.837	-17.824	0.695
	NM_002699	-1.180	-1.968	83.229
	NM_144701	-6.254	-9.691	-13.893
	NM_000844	-0.045	-0.128	0.061
	NM_013372	-0.042	-0.020	-0.030
Cardiovascular disease	NM_001242525	0.139	0.230	0.211
	NM_021977	-0.058	-0.050	-0.056
	NM_005562	-13.819	-47.359	-3.500
	NM_020469	-0.003	-0.002	0.002
	NM_020469	-0.003	-0.001	0.002
Gastrointestinal disturbance	NM_003121	-0.070	-0.031	-0.011
	NM_001142615	-0.133	-0.006	-0.020
	NM_001131027	0.009	-0.011	0.004
	NM_001131027	0.009	-0.011	0.004
	NM_144701	-92.938	204.027	64.581
Immune disease	NM_001242462	-0.032	-0.008	-0.034
	NM_000369	0.005	0.003	-0.005
	NM_145648	-0.005	-0.005	-0.006
	NM_144701	-6.254	-9.691	-13.893
	NM_000168	0.012	-0.016	0.007
Infection	NM_025236	0.001	-0.007	0.006
	NM_144701	-92.938	204.027	64.581
	NM_001242525	-0.023	-0.020	0.012
	NM_020469	-0.003	-0.002	0.002
	NM_004589	0.023	-0.047	0.016

Lifestyle-related disease	NM_006193	-0.016	-0.014	0.019
	NM_002670	-0.105	0.271	0.529
	NM_005921	-0.636	-23.812	-21.571
	NM_130438	0.795	0.069	0.179
	NM_006023	-0.223	-17.487	-6.032
Neuro degeneration	NM_014510	0.045	0.077	0.034
	NM_001256026	0.000	-0.024	-0.029
	NM_001134285	0.033	-0.166	0.015
	NM_001199214	0.034	-0.025	0.021
	NM_000844	-0.045	-0.128	0.061
Renal failure	NM_000099	0.003	0.013	-0.002
	NM_001008693	0.011	0.014	0.040
	NM_001242525	-0.023	-0.020	0.012
	NM_198098	0.048	-0.072	-0.333
	NM_001134404	0.002	0.006	0.011
Respiratory	NM_000744	-0.002	0.002	-0.001
	NM_006011	-0.001	-0.006	-0.003
	NM_182899	0.000	-0.002	0.002
	NM_004136	-0.065	0.109	0.223
	NM_006947	0.012	0.011	0.010
Skin	NM_144701	-92.938	204.027	64.581
	NM_001242525	-0.023	-0.020	0.012
	NM_002187	-36.212	-22.482	-10.731
	NM_052836	-0.170	-0.085	0.049
	NM_017637	0.001	-0.010	-0.009
Tumor	NM_022841	-0.116	-0.016	0.198
	NM_001142615	-0.133	-0.006	-0.020
	NM_005602	-12.376	-3.373	-1.087
	NM_018833	-0.011	0.007	-0.005
	NM_005921	-7.164	8.330	6.650

x shows number of G derived from DNS.
The maximum (red) and the minimum (blue) values of average of EFTSCs were represented

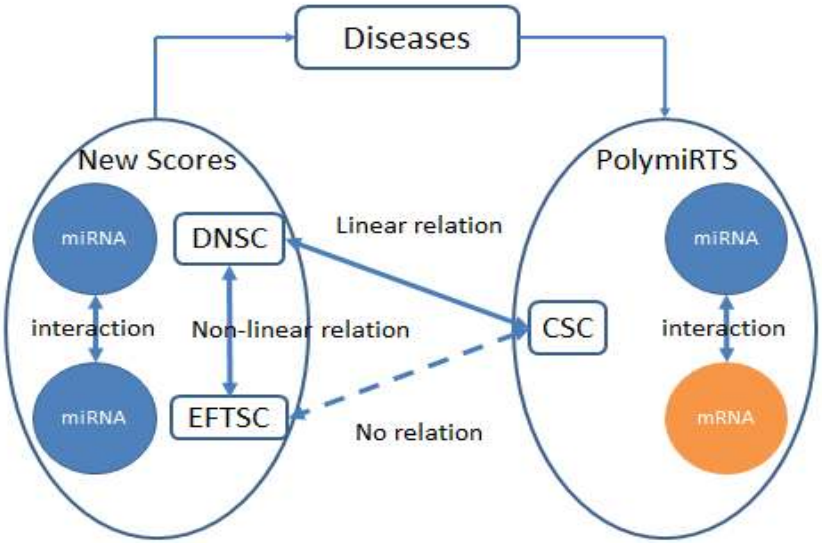

Fig. 5. Scheme of relation between CSC, DNSC and EFTSC

Genome-wide association studies (GWAS) have identified miRNA and SNPs of target implicated in complex human traits and disease, therefore the same non-linear regression analysis as above was performed in cardiovascular disease Top 5 target SNPs, HLA-DPA1 tv3, SLC22A3, LAMC2 tv1, ABO (Venous thromboembolism; yellow) and ABO (Coronary heart disease; blue) (Fig. 4E). Other 11 phenotypes, Age-related disease (A), bone and muscle (B), gastrointestinal disturbance (C), immune disease (D), infection (E), lifestyle-related disease (F), neurodegeneration (G), renal failure (H), respiratory disease (I), skin disease (J) and tumors (K), were also shown in Fig. S4(A-K). These data show that EFTSCs was related with DNSCs in non-linear regression and miRNA/miRNA multi-interaction on this algorithmic function could specifically discern among each disease phenotype from one to another without CSCs.

4. DISCUSSION

Recently, miRNA regulatory networks and miRNA-related SNPs have been studied intensely to understand their role in human disease [19,20]. A GWAS was conducted to reveal associations between miRNAs and disease [21]. In this study, we used PolymiRTS, which contains information about miRNAs and polymorphisms in their targets. PolymiRTS connects numerous disease with SNPs in pre-miRNAs, pri-miRNAs, miRNA promoters and miRNA targets [13]. SNPs in the miRNA genes and in their 3'UTR mRNA targets are largely diverse among individuals, and cause various phenotypes and disease. In our model experiments, we used the PolymiRTS database, because according to GWAS, SNPs in target sites are associated with disease. Role of these genetic traits has been confirmed using luciferase-based gain- and loss-of-function assays *in vitro* [19,22], by comparative analysis of the human genome, and a network-based experiment has recently revealed the target miRNAs (miR-943 and miR-571) for the therapy of hepatocellular carcinoma [23]. Furthermore, based on a functional assay using a miRNA lentivector library, the tamoxifen responsive miRNA has been identified as target in breast cancer using the genome-integrated pre-miRNA forced expression assay [24]. This suggests that the role of SNPs in the 3'UTR are identified with gain- and loss-of-function models in humans, and multiple parameters of miRNAs and their targets are essential in the diagnosis, treatment and prognosis of disease. In addition, SNPs in miRNA targets might predict miRNA function; therefore, pharmacogenomics and molecular epidemiology can utilize these results. GWAS revealed disease-related genes, which are related or not related to various biological pathways and mechanisms. We hypothesized that the latter case could be explained with miRNA/miRNA interactions, because almost of all biological events are controlled by miRNAs. For instance, there is a strong association between DNS and CSC values of GRM7 of Parkinson's disease. GRM7 can modulate

neurotransmitter release and neuronal excitability. Furthermore, GRM7 controls neural differentiation via the phosphorylation of CREB and regulation of YAP expression [25]. Therefore, according to GWAS, GRM7 is linked to bipolar [26], depression [27], hyperactive disorder [28], schizophrenia [29] and age-related hearing loss [30]. On the contrary, ESRRG is related to neurodegeneration; however, according to the literature, ESRRG is mainly implicated in the energy-balance of the whole body [31], and function of ESRRG in neurotransmission remains unknown. In the case of this GWAS, our data shows that ESRRG might function via miRNA/miRNA multiple interactions. Thus, our findings suggest that miRNA/miRNA multiple interactions are crucial in human disease and sufficient for the prediction of diagnosis and prognosis (see Fig. 6).

Torus RNA could be advantageous for biological prevalence because it can serve as template for rolling circle replication and be stable due to be resistant to exonucleases [32]. In our experiments, it can be simulated that torus model of miRNA can transmit genetic information among miRNAs therefore, the circular type of RNA might have an important role for its function to architect the mechanisms of tuning of miRNA. Quite recently, it has been reported that natural circular RNA were identified in human cells and the circular RNA (1,400 nts) can bind to miR-7 as the sponge [33]. Further Y RNA is known as a family of non-coding and a natural circular RNA [34], and human Y3 and Y5 (25 nts each) were annotated as miR-1979 and miR-1975 in miRBase, respectively. Artificially, the repetitive circular RNAs (approximate 14 nts) are catalyzed by polymerase from ribozymes and 34 nts RNA were made as circular RNA by using a template-directed non-enzymatic ligation [35]. These results indicated that natural mobile torus miRNA could be bio-generated and have a function to transmit gene information. Further, circular RNA has been related with cancer [36]. Intriguingly, above miR-1979 and miR-1975 are circulating miRNA, and as biomarkers, miR-1979 is associated with multiple sclerosis [37] and chronic congestive heart failure [38]. In addition, miR-1975 is implicated in liver cancer [39], suggesting that the circulating circular miRNA genes would have some function to induce human disease, therefore, DNSC and EFTS scorings under tours condition are suitable for human disease prediction to be relevant to GWAS.

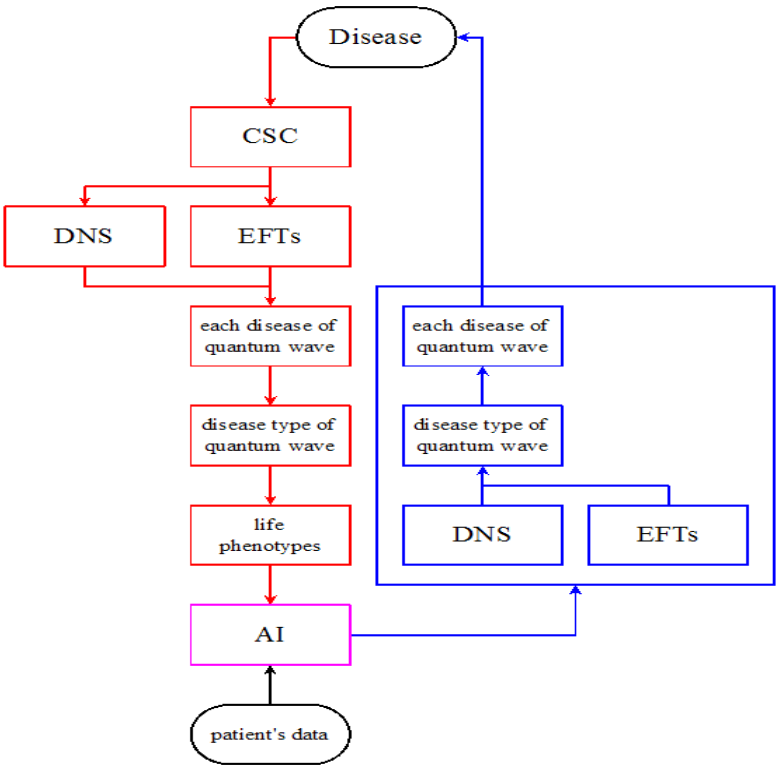

Fig. 6. The future prospecting model

We classified human disease with algorithms based on electrodynamics and quantum energy of miRNA nucleotides. EFTS based on electrodynamics corresponds to nucleotide changes in miRNAs, such as keto-enol tautomerism [40], changes induced by environmental stress, including ultraviolet rays [41] and A/I RNA editing [42]. On the contrary, DNS corresponds to the presence of G bases in miRNAs but not tautomerism. Guanine generate G-quartets [43] or scale of the fish caused by changes in the magnetic field [44]. In addition, miRNA SNPs changed to guanine are more effective [45]. Accordingly, G-dependent miRNA/miRNA interactions, based on the miR-ket code, are important factors in the association of miRNAs and human disease [46]. While CSC and EFTS were not related, CSC correlated with DNS. Therefore, guanine bases in miRNAs are often associated with disease-related polymorphisms. Furthermore, in the targets, approximately 40% of DNS values have a linear relationship with CSC. Therefore, DNS might be a useful tool to remove false positive data from a large miRNA dataset in targets.

As a miRNA contain approximately 22 nucleotides, the DNS value can only have 276 varieties. However, corresponding to Watson-Crick base pair and wobble base pair, the EFTS value can have $2^{131}+2^{65}$ varieties. We found that EFTS convergently has a non-linear relationship with DNS. The non-linear regression analysis with a Fourier transformation showed that each disease can be represented with a specific non-linear curve. Because in classical mechanics all physical events can be described with specific wave properties using quantum mechanics, our results would be rational to physical criteria. Thus, EFTS (related to classical mechanics) and DNS (related to quantum mechanics) had a non-linear relationship, suggesting that each disease is visualized using specific wave properties. In addition, using non-linear curves without CSC, phenotype of human disease can be identified. Therefore, human disease may be predicted by the miRNA/miRNA interaction as miRNA memory only.

As the calculation of EFTS and DNS values is still problematic, further research is necessary. Firstly, when we set EFTS, atoms that form a Watson–Crick base pair [47] or wobble base pair [48] were selected as active ones. However, nucleic acids can also form a Hoogsteen base pair [49]. Hoogsteen base pairs are related to the G-quartet structure and Fragile X mental retardation protein (FMRP) nucleic acid chaperone has facilitated miRNA assembly inviting recognition of G-quartet structures on target mRNAs [50]; therefore, EFTS calculations have to be set up for Hoogsteen base pairs. Secondly, although we presented the relationship between miRNA/miRNA interactions and disease based on GWAS, the expression levels of miRNAs were not considered, because miRNA-mRNA binding sites were identified with direct mapping experiments such as cross linking, ligation and sequencing of hybrids (CLASH) [51]. Therefore, integration of comparative miRNA qualitative expression levels might improve the performance of the model. Further progression was necessary for precision scoring.

5. CONCLUSION

Neo-scores based on the quantum and electrodynamic data of the miRNA/miRNA interaction, DNS and EFTS, respectively, is shown in Fig. 5. DNS was correlated with CSC using PolymiRTS data to evaluate the relationship between miRNAs and protein coding genes invade in 149 human disease. Because EFTS was mathematically functioned into DNS, function of DNS to EFTS was integrated for disease prediction on CSC. Furthermore, in this context, miRNA/miRNA interactions in the algorithmic function might be applied for specific discernment of disease with the miRNA/target interaction complex. Thus, miRNA/miRNA interactions as miRNA disease memory may have an important role in the *a priori* disease control of human health.

Utility of neo scores is shown in Fig. 6. Artificial Intelligence (AI) combined with the EFTS/DNS-based prediction method might help in the diagnosis of disease. From a technical point of view, our method might improve the prediction of miRNA/miRNA interactions with AI by using more accurate information.

CONSENT

It is not applicable.

ETHICAL APPROVAL

It is not applicable.

SUPPLEMENTAL INFORMATION

Supplemental Information includes Extended Experimental Procedures, seven figures, and three tables and can be found

with this article online at http://mirna-academy.org/database/supplemental.html.

COMPETING INTERESTS

Authors have declared that no competing interests exist.

REFERENCES

1. Yang C, Tang R, Ma X, Wang Y, Luo D, Xu Z. Tag SNPs in long non-coding RNA H19 contribute to susceptibility to gastric cancer in the chinese han population. Oncotarget; 2015.
2. Ebert MS, Sharp PA. Roles for microRNAs in conferring robustness to biological processes. Cell. 2012;149(3):505-524.
3. Ambros V. The functions of animal microRNAs. Nature. 2004;431(7006):350-355.
4. Jung IL, Ryu M, Cho SK, Shah P, Lee JH, Bae H, et al. Cesium toxicity alters microRNA processing and AGO1 expressions in *Arabidopsis thaliana*. PLoS One. 2015;10(5):e0125514.
5. Hill CG, Jabbari N, Matyunina LV, McDonald JF. Functional and evolutionary significance of human microRNA seed region mutations. PLoS One. 2014;9(12): e115241.
6. Kume H, Hino K, Galipon J, Ui-Tei K. A-to-I editing in the miRNA seed region regulates target mRNA selection and silencing efficiency. Nucleic Acids Res. 2014;42(15): 3-8.
7. Granados-Riveron JT, Aquino-Jarquin G. Does the linear Sry transcript function as a ceRNA for miR-138? The sense of antisense. F1000 Research. 2014;90(0): 2012-2014.
8. Salmena L, Poliseno L, Tay Y, Kats L, Pandolfi PP. A ceRNA hypothesis: The rosetta stone of a hidden RNA language? Cell. 2011;146(3):353-358.
9. Yu J, Tan Q, Deng B, Fang C, Qi D, Wang R. The microRNA-520a-3p inhibits proliferation, apoptosis and metastasis by targeting MAP3K2 in non-small cell lung cancer. Am J Cancer Res. 2015;5(2):802-811.
10. Garcia DM, Baek D, Shin C, Bell GW, Grimson A, Bartel DP. Weak seed-pairing stability and high target-site abundance decreases the proficiency of lsy-6 and other miRNA's. Nat Struct Mol Biol. 2011;18(10):1139-1146.
11. Griffiths-Jones S, Grocock RJ, van Dongen S, Bateman A, Enright AJ. miRBase: microRNA sequences, targets and gene nomenclature. Nucleic Acids Res. 2006; 34(Database issue):D140-D144.
12. Smigielski EM, Sirotkin K, Ward M, Sherry ST. dbSNP: A database of single nucleotide polymorphisms. Nucleic Acids Res. 2000;28(1):352-355.
13. Bhattacharya A, Ziebarth JD, Cui Y. PolymiRTS Database 3.0: Linking polymorphisms in microRNAs and their target sites with human diseases and biological pathways. Nucleic Acids Res. 2014;42(D1):86-91.
14. Delay C, Dorval Vã©, Fok A, Grenier-Boley B, Lambert J-C, Hsiung G-Y, et al. MicroRNAs targeting nicastrin regulate Aî^2 production and are affected by target site polymorphisms. Front Mol Neurosci. 2014; 7:1-7.
15. Jia M, Yang B, Li Z, Shen H, Song X, Gu W. Computational analysis of functional single nucleotide polymorphisms associated with the CYP11B2 gene. PLoS One. 2014;9(8).
16. Fujii YR. The RNA gene information: retroelement-microRNA entangling as the RNA quantum code. Methods Mol Biol. 2013;936:47-67.
17. Fujii YR. RNA wave for the HIV therapy : foods , stem cells and the RNA information gene. World J AIDS. 2013;3:131-146.
18. Fujii YR. RNA genes: retroelements and virally retroposable microRNAs in human embryonic stem cells. Open Virol J. 2010; 4:63-75.
19. Chin LJ, Ratner E, Leng S, Zhai R, Nallur S, Muller R, et al. A SNP in a let-7 microRNA complementary site in the KRAS 3′UTR Increases non-small cell lung cancer risk. Cancer Res. 2008;68(20): 8535-8540.
20. Plaisier CL, Pan M, Baliga NS. A miRNA-regulatory network explains how dysregulated miRNAs perturb oncogenic processes across diverse cancers. Genome Res. 2012;22(11):2302-2314.
21. Goulart LF, Bettella F, Sønderby IE, Schork AJ, Thompson WK, Mattingsdal M, et al. MicroRNAs enrichment in GWAS of complex human phenotypes. BMC Genomics. 2015;16(1).
22. Gong J, Tong Y, Zhang HM, Wang K, Hu T, Shan G, et al. Genome-wide identification

of SNPs in microRNA genes and the SNP effects on microRNA target binding and biogenesis. Hum Mutat. 2012;33(1):254-263.

23. Yu F, Shen X-Y, Fan L, Yu Z-C. Genome-wide analysis of genetic variations assisted by ingenuity pathway analysis to comprehensively investigate potential genetic targets associated with the progression of hepatocellular carcinoma. Eur Rev Med Pharmacol Sci. 2014;18: 2102-2108.
24. Ujihira T, Ikeda K, Suzuki T, Yamaga R, Sato W, Horie-Inoue K, et al. MicroRNA-574-3p, identified by microRNA library-based functional screening, modulates tamoxifen response in breast cancer. Sci Rep. 2015;5:7641.
25. Xia W, Liu Y, Jiao J. GRM7 regulates embryonic neurogenesis via CREB and YAP. Stem Cell Reports. 2015;4:1-16.
26. Alliey-Rodriguez N, Zhang D, Badner J a, Lahey BB, Zhang X, Dinwiddie S, et al. Genome-wide association study of personality traits in bipolar patients. Psychiatr Genet. 2011;21(4):190-194.
27. Shyn SI, Hamilton SP. The genetics of major depression: Moving beyond the monoamine hypothesis. Psychiatr Clin North Am. 2010;33(1):125-140.
28. Elia J, Glessner JT, Wang K, Takahashi N, Shtir CJ, Hadley D, et al. Genome-wide copy number variation study associates metabotropic glutamate receptor gene networks with attention deficit hyperactivity disorder. Nat Genet. 2012;44(1):78-84.
29. Choi KH, Zepp ME, Higgs BW, Weickert CS, Webster MJ. Expression profiles of schizophrenia susceptibility genes during human prefrontal cortical development. J Psychiatry Neurosci. 2009;34(6):450-458.
30. Friedman R a, Van Laer L, Huentelman MJ, Sheth SS, Van Eyken E, Corneveaux JJ, et al. GRM7 variants confer susceptibility to age-related hearing impairment. Hum Mol Genet. 2009;18(4):785-796.
31. Byerly MS, Al Salayta M, Swanson RD, Kwon K, Peterson JM, Wei Z, et al. Estrogen-related receptor β deletion modulates whole-body energy balance via estrogen-related receptor γ and attenuates neuropeptide Y gene expression. Eur J Neurosci. 2013;37(7):1033-1047.
32. Lasda E, Parker ROY. Circular RNAs : Diversity of form and function. RNA. 2015;20:1829-1842.
33. Hansen TB, Kjems J, Damgaard CK. Circular RNA and miR-7 in cancer. Cancer Res. 2013;73(18):5609-5612.
34. Nicolas FE, Hall AE, Csorba T, Turnbull C, Dalmay T. Biogenesis of y RNA-derived small RNAs is independent of the microRNA pathway. FEBS Lett. 2012; 586(8):1226-1230.
35. Diegelman AM, Kool ET. Generation of circular RNAs and trans-cleaving catalytic RNAs by rolling transcription of circular DNA oligonucleotides encoding hairpin ribozymes. Nucleic Acids Res. 1998; 26(13):3235-3241.
36. Hansen TB, Jensen TI, Clausen BH, Bramsen JB, Finsen B, Damgaard CK, et al. Natural RNA circles function as efficient microRNA sponges. Nature. 2013; 495(7441):384-388.
37. Siege SR, MacKenzie J, Chaplin G, Jablonski NG, Griffiths L. Circulating microRNAs involved in multiple sclerosis. Mol Biol Rep. 2012;39(5):6219-6225.
38. Cakmak HA, Coskunpinar E, Ikitimur B, Barman H, Karadag B, Tiryakioglu N, et al. The prognostic value of circulating microRNAs in heart failure: Preliminary results from a genome-wide expression study . J Cardiovasc Med. 2015;16(6).
39. Lin L, Lin Y, Jin Y, Zheng C. Microarray analysis of microRNA expression in liver cancer tissues and normal control. Gene. 2013;523(2):158-160.
40. Szczepaniak K, Szczesniak M. Matrix isolation infrared studies of nucleic acid constituents : Part 4. Guanine and 9-methylguanine monomers and their keto—enol tautomerism. 1987;156(1-2):29-42.
41. Hu J, Adar S, Selby CP, Lieb JD, Sancar A. Genome-wide analysis of human global and transcription-coupled excision repair of UV damage at single-nucleotide resolution. GENES Dev. 2015;29:948-960.
42. Paz-Yaacov N, Levanon EY, Nevo E, Kinar Y, Harmelin A, Jacob-Hirsch J, et al. Adenosine-to-inosine RNA editing shapes transcriptome diversity in primates. Proc Natl Acad Sci U S A. 2010;107(27):12174-12179.
43. Williamson JR, Raghuraman MK, Cech TR. Monovalent cation-induced structure of telomeric DNA: The G-quartet model. Cell. 1989;59(5):871-880.
44. Iwasaka M, Mizukawa Y. Light reflection control in biogenic micro-mirror by

diamagnetic orientation. Langmuir. 2013; 29(13):4328-4334.
45. Wang Z, Sun X, Wang Y, Liu X, Xuan Y, Hu S. Association between miR-27a genetic variants and susceptibility to colorectal cancer. Tumor Biol. 2014;35(3): 2151-2156.
46. Fujii YR. Formulation of new algorithmics for miRNAs. Open Virol J. 2008;2:37-43.
47. Watson JD, Crick FHC. Molecular structure of nucleic acids. Nature. 1953;171(4356): 737-738.
48. Crick FH. Codon--anticodon pairing: The wobble hypothesis. J Mol Biol. 1966; 19(2):548-555.
49. Hoogsteen K. The crystal and molecular structure of a hydrogen-bonded complex between 1-methylthymine and 9-methyladenine. Acta Cryst. 1963;16:907-916.
50. Plante I, Provost P. Hypothesis: A role for fragile X mental retardation protein in mediating and relieving microRNA-guided translational repression? J Biomed Biotechnol. 2006;2006:1-7.
51. Kudla G, Granneman S, Hahn D, Beggs JD, Tollervey D. Cross-linking, ligation, and sequencing of hybrids reveals RNA-RNA interactions in yeast. Proc Natl Acad Sci USA. 2011;108(24):10010-10015.

Peer-review history:
The peer review history for this paper can be accessed here:
http://sciencedomain.org/review-history/12275